2nd International Symposium on Magnetic Beaing
July 12-14, 1990, Tokyo, Japan

PERFORMANCE COMPARISON BETWEEN CENTRALIZED AND DECENTRALIZED CONTROL OF THE JEFFCOTT ROTOR

P. LAROCCA, D. FERMENTAL, E. CUSSON
The Charles Stark Draper Laboratory, Inc.
555 Technology Square, Cambridge, MA, USA

Abstract

Decentralized control is a typical strategy for controlling a rotating shaft/rotor using magnetic bearing actuators. It is often chosen for its simplicity of design and ease of implementation in analog circuitry. However, in high performance systems where high bandwidth is required, decentralized control may not be appropriate. This paper numerically analyzes the decentralized control of a Jeffcott rotor and shows that system bandwidth decreases as rotor rotational velocity increases. The paper then compares the performance of a centralized and a decentralized controllerto illustrate that the higher bandwidth achieved using centralized control has significant performance advantages over decentralized control.

1. Introduction

Decentralized control of magnetic bearing systems has been the subject of much research in both the commercial and academic communities. A review of magnetic bearing literature reveals that decentralized control exhibits adequate performance while being simple in design and implementation [1,2]. Most applications concern fixed platform land based rotating systems whose primary disturbances are gravity and mass unbalance loading. In such applications, high system bandwidth is not required to maintain stability and special means are used to allow operation beyond shaft critical speeds.

This paper addresses the bandwidth limitations imposed by using decentralized control and suggests that for systems operating in a moving platform environment with a dynamic disturbance envelope, such as a high performance jet engine, decentralized control may not meet performance requirements.

Numerical analysis is used to determine closed loop bandwidth of a system which consists of a rotating shaft/rotor with a four axis radial control scheme, each axis having a position and velocity sensor and P-D controller. The individual controllers are decoupled (i.e. decentralized control).

The rotor model used is the Jeffcott rotor. In this model, the rotor is taken to be a mass exhibiting inertia attached to a massless shaft characterized by stiffness and damping. The Jeffcott model is both controllable and observable for all rotational rates. The magnetic bearing actuators are assumed to be linear force devices and are not considered in the analysis. Mass unbalance and gravity are also ignored.

A decentralized controller has eight feedback gains, a number that is insufficient to independently place the twelve plant poles. This paper uses numerical methods to show that at high plant rotation rates, stable decentralized control dictates low control gains and, as a result, severely limits the allowed system bandwidth.

Since the Jeffcott rotor is both controllable and observable, a centralized control scheme will allow unrestricted system bandwidth via independent pole placement. This implies that any desired performance can theoretically be achieved. Since the system poles can be placed at any desired location, the problem of critical speeds does not arise.

The paper first presents the Jeffcott rotor model in a normalized state space form. Normalization allows the plant to be characterized by five independent ratios. A decentralized feedback gain matrix [G] is introduced and the closed loop system

is formed. *Decentralized control requires velocity* sensors or velocity estimators. The $[G]$ matrix is combined with the feedforward $[D]$ matrix, created by the velocity sensors, to form a new $[g]$ matrix which is combined with the $[A, B, C]$ system matrices to complete the closed loop system. In order to facilitate calculations, the rotor is taken as a sphere at the center of a massless rod and, because of symmetry, the four P-D controllers are assumed to be identical.

The numerical analysis consists of calculating stability regions of decentralized control gains for various rotational operating speeds. The results show that as the rotational rate increases, the stability region decreases and that the gains are limited to a region of lower values. As a consequence of the *reduced gains, system* bandwidth decreases with increasing rotational velocity. This conclusion is supported by bandwidth estimations from closed loop pole locations.

A performance comparison is made between a decentralized controller and a centralized, optimal full state feedback controller. The comparison is based on step response and disturbance rejection simulations done under identical operating conditions.

2 Jeffcott Rotor Model

To generalize results, the Jeffcott rotor model is expressed in normalized form. That is, it is expressed in terms of dimensionless ratios and therefore made dimensionless. The model is presented in state space form, and no derivation is included. For a Lagrangian based derivation, see [3], for a Newtonian based derivation, see [4].

The Jeffcott model consists of a rotor on a flexible shaft which is characterized by stiffness and damping terms. The magnetic bearing actuators are not considered and the Jeffcott model accepts force inputs. The plant can be described in twelve states. Four states describe the rotor positions and velocities in the Y-Z plane, the X-axis is the axis of rotation. Four states describe pitch and yaw angle and rates and the remaining four states describe the amount of bending a shaft has incurred. Figure 1 illustrates this concept for the Y-axis.In the figure, Y_r defines the Y-axis rotor position, ξ_2 defines the pitch angle, Y_1 represents the Y-axis position sensor output at bearing 1. The Y_1 position is comprised of two parts, Y_{S1} which represents the position of an stiff shaft deflection, and D_{Y1} which represents the amount that the shaft has bent on the left side of the rotor. ω_x is the rotational velocity about the X-axis.

The complete set of system matrices in normalized form appear in Appendix A. The plant state vector is defined as $[\mathbf{x}]^t =$

$$[Y_r, \xi_2, Z_r, \xi_1, \dot{Y}_r, \dot{\xi}_2, \dot{Z}_r, \dot{\xi}_1, D_{Y1}, D_{Z1}, D_{Y2}, D_{Z2}].$$

The plant input vector is defined as

$$[\mathbf{u}]^t = [F_{Y1}, F_{Z1}, F_{Y2}, F_{Z2}]$$

and the state output vector,shaft position and velocity information at each bearing, is defined as

$$[\mathbf{y}]^t = [Y_1, Z_1, Y_2, Z_2, \dot{Y}_1, \dot{Z}_1, \dot{Y}_2, \dot{Z}_2].$$

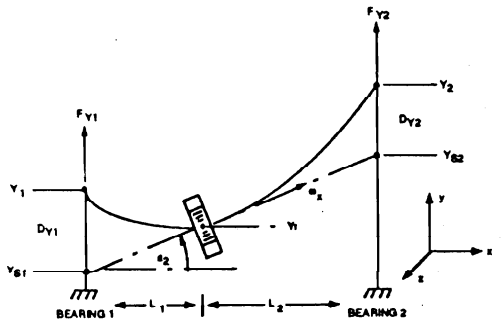

Figure 1: Flexible Shaft Definitions

The model is normalized by defining basic system units as follows:

1 unit of length	=	L1 meters
1 unit of time	=	$\frac{1}{S_0}$ seconds
1 unit of mass	=	M kg

where L1 is the distance from magnetic bearing 1 to the rotor center, M is the mass of the rotor, and S_0 is the ratio of shaft stiffness to damping in $\sec^{-1}$. Using these as basic units, a unit of force can now be defined as

1 unit of force = M*L1*S_0^2 newtons.

The damping factor associated with the shaft between the mass and bearing 1 is $B1$. Its normalized value is $\frac{1}{v}$ and is defined as

$$\frac{1}{v} = \frac{B1/M}{S_0}.$$

Since $(B1/K1) = S_0$, where $K1$ is the shaft stiffness constant for the same shaft section, the normalized value of $K1$ is $\frac{1}{v}$ as well. The radial inertia of the rotor, Jr, has the normalized value $\frac{1}{m}$ with

$$\frac{1}{m} = \frac{J_r}{M*L1^2}.$$

and to complete the normalization, three other ratios are defined as

$$\begin{aligned} r &= \frac{L2}{L1} = \frac{B2}{B1}\,\frac{K2}{K1} \\ w &= \frac{\omega_x}{S_0} \\ a &= \frac{J_a}{J_r} * w \end{aligned}$$

where $\omega_x$is the angular velocity of the rotor and Ja is the axial rotor inertia.

To provide meaning to these normalizations, we will present a set of plant parameters in standard MKS units and their normalized equivalents in Table 1. to them:

Parameter	Physical units	Normalized units
Mass M	100 Kg	1
Shaft stiffness K1	$4 \times 10^6\ \frac{Newton}{meter}$	1/100
Shaft damping B1	$2000\ \frac{Newton-sec}{meter}$	1/100
Length L1	1 $meters$	1
Inertia Jr	1 $Kg - meter^2$	1/100
S_0 = K1/B1	2000 sec^{-1}	1

Table 1. Plant Parameters

3 Numerical Analysis

The system equations in standard state space form are

$$\begin{aligned} \dot{\mathbf{x}} &= A\,\mathbf{x} + B\,\mathbf{u} \\ \mathbf{y} &= C\,\mathbf{x} + D\,\mathbf{u} \\ \mathbf{u} &= -G\,\mathbf{y} \end{aligned}$$

with A, B, C and D given in the Appendix and normalized G being

$$\begin{bmatrix} G11 & 0 & 0 & 0 & G21 & 0 & 0 & 0 \\ 0 & G11 & 0 & 0 & 0 & G21 & 0 & 0 \\ 0 & 0 & G12 & 0 & 0 & 0 & G22 & 0 \\ 0 & 0 & 0 & G12 & 0 & 0 & 0 & G22 \end{bmatrix}.$$

We assume the plant is completely symmetric so that $G11 = G12$ and $G21 = G22$.

The feedforward matrix D and the feedback matrix G can be combined to form a single feedback matrix g as follows. Substituting in for $\mathbf{y}$, $\mathbf{u}$ becomes

$$\mathbf{u} = -\,GC\,\mathbf{x} - GD\,\mathbf{u}.$$

Solving for $\mathbf{u}$ yields

$$\mathbf{u} = -\,[\mathrm{I} + GD]^{-1}\,GC\,\mathbf{x}.$$

That is

$$\begin{aligned} \mathbf{u} &= -\,gC\,\mathbf{x} \text{ where} \\ g &= -\,[\mathrm{I} + GD]^{-1}\,G. \end{aligned}$$

Thus the system can be modeled with the four matrices $[A]$, $[B]$, $[C]$, $[g]$, and the closed loop system matrix becomes

$$A_{cl} = A - BgC,$$

where g is

$$\begin{bmatrix} g1 & 0 & 0 & 0 & g2 & 0 & 0 & 0 \\ 0 & g1 & 0 & 0 & 0 & g2 & 0 & 0 \\ 0 & 0 & g1 & 0 & 0 & 0 & g2 & 0 \\ 0 & 0 & 0 & g1 & 0 & 0 & 0 & g2 \end{bmatrix}.$$

For the plant parameters of Table 1 and with $r = 1$ and with $a = w$, so that, $m = 100$, $v = 100$, numerical analysis was used to determine the stability region of the gains $g1$ and $g2$ as a function of the normalized rotational velocity, w.

The objective of the analysis is to determine, for a given w, the range of gains over which the system is stable and to determine the maximum achievable bandwidth for that w. Bandwidth can be defined in many ways. Here, however, for all w there is a pole pair closer to the origin than any other system pole, and it is reasonable to take for the system bandwidth the real part of these poles, since the inverse of this is a measure of system settling time.

The stability of the closed loop system was tested for the logarithmically spaced gain vectors

$[g1(i), g2(j)]$ in the range of 10^{-5} to 10^{3}. This was done for selected values of w. Figure 2 shows the composite stability regions in the $(g1, g2)$ plane. As the figure shows, the stability region is a maximum at small w, and becomes progressively smaller as w increases. Further, the gains are limited to lower values. This suggests the system bandwidth must decrease for increasing w. The bandwidth results are summarized in Table 2 which contains the w of interest, the maximum bandwidth at that rate, and the gains which created that bandwidth. Note that the table is in scaled units.

w	$g1$	$g2$	Bandwidth
0.01	1000	1000	4.92×10^{-1}
0.02	1000	1000	4.87×10^{-1}
0.03	1000	1000	1.57×10^{-1}
0.04	1.00	8.90×10^{-1}	7.08×10^{-2}
0.05	1.00	8.90×10^{-1}	6.26×10^{-2}
0.06	1.00	8.90×10^{-1}	4.73×10^{-2}
0.07	4.13×10^{-4}	8.49×10^{-3}	4.55×10^{-2}
0.08	4.13×10^{-4}	8.49×10^{-3}	4.55×10^{-2}
0.09	4.13×10^{-4}	8.49×10^{-3}	4.54×10^{-2}
0.10	4.13×10^{-4}	8.49×10^{-3}	4.54×10^{-2}
0.14	4.13×10^{-4}	8.49×10^{-3}	4.54×10^{-2}
0.20	4.13×10^{-4}	8.49×10^{-3}	4.52×10^{-2}
0.30	4.13×10^{-4}	8.49×10^{-3}	4.52×10^{-2}
0.40	4.13×10^{-4}	8.49×10^{-3}	4.52×10^{-2}
0.50	4.13×10^{-4}	8.49×10^{-3}	4.52×10^{-2}

Table 2. Decentralized Control Summary

To provide meaning to the scaled units, w = .01 rads/pseudoseconds (psec) corresponds to 20 rads/sec or a 3.18 Hz rotational rate and the bandwidth of .49 rads/psec correspond to 980 rads/sec or a 156 Hz bandwidth. At w = .1 rads/psec, a 31.8 Hz rotational rate the system bandwidth falls to .0454 rads/psec or 14.5 Hz bandwidth. Clearly, as the rotational velocity increases, the system bandwidth decreases. It must do so for decentralized control.

4 Performance Comparison

In order to illustrate the consequence of bandwidth limitations imposed by decentralized control, a comparison of performance will be made using both centralized and decentralized controllers operating on the same plant under the same test conditions. Step

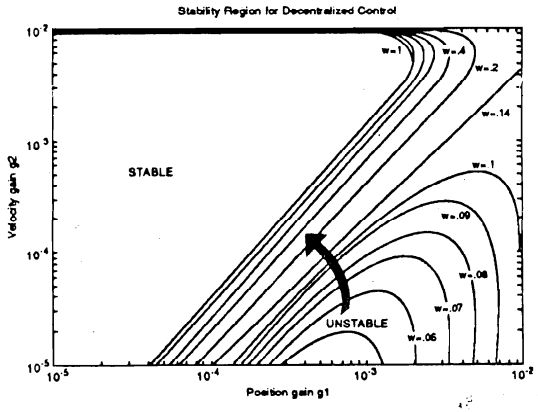

Figure 2: Composite stability regions

response simulations are typically used as performance measures in control system evaluations and were used here. Additionally, d.c. disturbance simulations were run to illustrate the rejection properties of both controllers.

The simulations were run using the normalized system, so time is expressed in pseudoseconds (psec) where 1 psec = 1/2000 sec. For the tests, the rotational velocity of the rotor was set at $\sqrt{.02}$ or .141 rads/psec. This corresponds to the plant resonant frequency, where $\omega_r^2 = 2K1/M$, or $w^2 = 2/v$. The gains for the decentralized controller are such that they provide the maximum possible bandwidth for a stable configuration. The gains used are $g_{position} = 4.132 \times 10^{-4}$ and $g_{velocity} = 8.49 \times 10^{-3}$. The decentralized closed loop bandwidth is dictated by the pole pair at -0.0454 $\pm 0.0666j$.

The centralized control system used is an optimal state feedback controller. Centralized control has additional degrees of control freedom which allows for complete and independent pole placement. Therefore, the resulting closed loop bandwidth is not limited, and can be made any value desired. For the purpose of comparison, it was made to be approximately 6 times the closed loop bandwidth of the maximum decentralized controller bandwidth. The centralized control closed loop bandwidth is dictated by the pole pair at -0.2869 $\pm 0.2754j$.

Figure 3 contains the closed loop frequency re-

sponses of the centralized and decentralized systems. The loop is measured from position command input to rotor position output. It clearly illustrates the increased bandwidth afforded by using a centralized control system.

A step response simulation of the two systems is shown in Figure 4. The command input is a step of 1.27×10^{-4} meters (5 mils) of rotor position in the Y axis. The time, in pseudoseconds, represents .1 seconds. The centralized controller response is close to ten times faster, with much less over-shoot. Figure 5 contains the rotor position when a d.c. disturbance to simulate gravity is applied. Again the centralized controller dramatically out-performs the decentralized controller. The time of response is much faster, but more importantly, the magnitude of the rotor displacement is 100 times less in the centralized control response. The decentralized control rotor may have exceeded its hard stop limit just from the application of gravity. In a jet engine application, the disturbance envelope can include load at up to ten times gravity [5] and clearly, a limited bandwidth decentralized control strategy is not adequate.

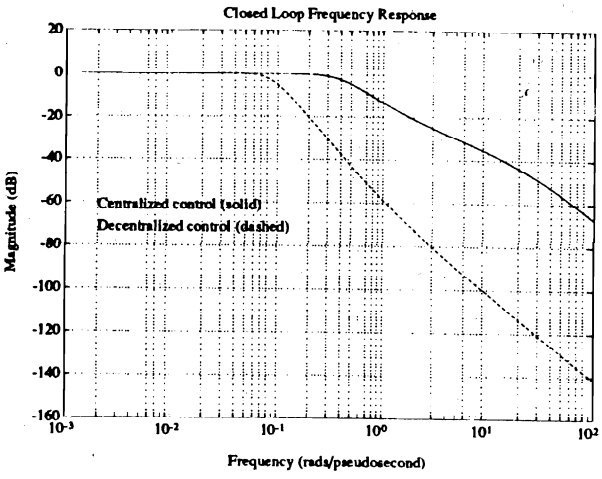

Figure 3: Closed loop frequency responses

5 Conclusion

A normalized version of the Jeffcott Rotor model was presented. Stability regions for decentralized control were determined as a function of rotor rotational velocity. From those stability regions, the maximum closed loop system bandwidth design was found, and the bandwidth and the associated decentralized controller gains were noted. It was shown that as the rotational velocity increased, the maximum bandwidth achievable decreased due to a decrease in the stability region of the decentralized control gains to lower and lower values. To quantify the lower bandwidth forced by the use of decentralized control, a high bandwidth, centralized control system was designed using optimal full state feedback techniques and a performance comparison between the two control systems was done under identical operating conditions. The centralized controller clearly has significant performance advantages over the decentralized controller in both step response and disturbance rejection tests.

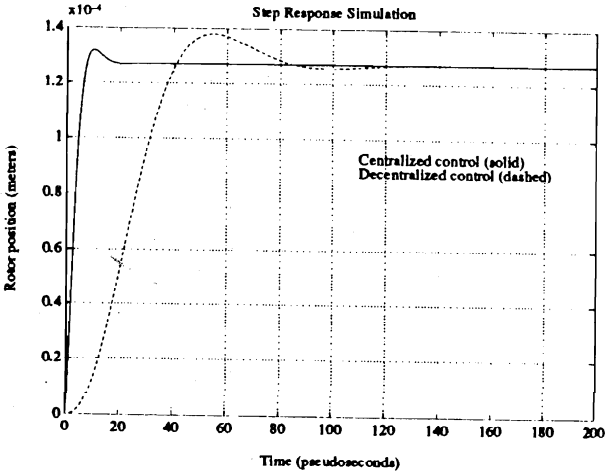

Figure 4: System step responses

References

[1] Schweitzer, G. and A. Traxler. **Design of Magnetic Bearings**. Proceedings of the International Symposium on Design and Synthesis, Tokyo, Japan, July, 1984.

[2] Blueler, H. and G. Schweitzer. **Dynamics of a Magnetically Suspended Rotor with Decentralized Control**. Applied Control and Iden-

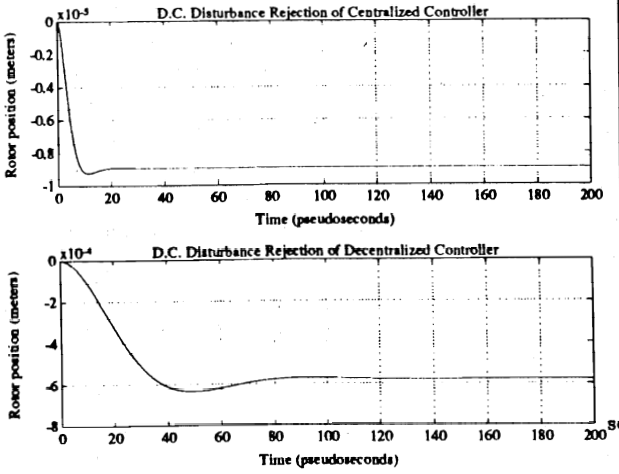

Figure 5: Gravity application responses

tification Symposium of the IASTED, Copenhagen, June,1983.

[3] McCallum, D. **Dynamic Modelling and Control of a Magnetic Bearing — Suspended Rotor System**, MIT SM Thesis, May, 1988.

[4] Fermental, D., P. LaRocca, and E. Cusson. **The Jeffcott Rotor: It's Decomposition and Control**. C.S. Draper Lab Report CSDL-P-2920, February, 1990.

[5] Pratt and Whitney Co. report FR-18022.

Appendix A

This appendix contains the system matrices in normalized form. The system is in the standard state space form

$$\dot{\mathbf{x}} = A\,\mathbf{x} + B\,\mathbf{u}$$
$$\mathbf{y} = C\,\mathbf{x} + D\,\mathbf{u}.$$

The state vector is defined as

$$[\mathbf{x}]^t = [Y_r, \xi_2, Z_r, \xi_1, \dot{Y}_r, \dot{\xi}_2, \dot{Z}_r, \dot{\xi}_1, D_{Y1}, D_{Z1}, D_{Y2}, D_{Z2}],$$

and the A matrix is

$$\begin{bmatrix}
0 & 0 & 0 & 0 & 1 & 0 & 0 & 0 & 0 & 0 & 0 & 0 \\
0 & 0 & 0 & 0 & 0 & 1 & 0 & 0 & 0 & 0 & 0 & 0 \\
0 & 0 & 0 & 0 & 0 & 0 & 1 & 0 & 0 & 0 & 0 & 0 \\
0 & 0 & 0 & 0 & 0 & 0 & 0 & 1 & 0 & 0 & 0 & 0 \\
0 & 0 & 0 & 0 & 0 & 0 & 0 & 0 & 0 & 0 & 0 & 0 \\
0 & 0 & 0 & 0 & 0 & 0 & 0 & a & 0 & 0 & 0 & 0 \\
0 & 0 & 0 & 0 & 0 & 0 & 0 & 0 & 0 & 0 & 0 & 0 \\
0 & 0 & 0 & 0 & 0 & -a & 0 & 0 & 0 & 0 & 0 & 0 \\
0 & 0 & 0 & 0 & 0 & 0 & 0 & 0 & -1 & -w & 0 & 0 \\
0 & 0 & 0 & 0 & 0 & 0 & 0 & 0 & w & -1 & 0 & 0 \\
0 & 0 & 0 & 0 & 0 & 0 & 0 & 0 & 0 & 0 & -1 & -w \\
0 & 0 & 0 & 0 & 0 & 0 & 0 & 0 & 0 & 0 & w & -1
\end{bmatrix}$$

The input vector is defined as

$$[\mathbf{u}]^t = [F_{Y1}, F_{Z1}, F_{Y2}, F_{Z2}]$$

so that [B] is

$$\begin{bmatrix}
0 & 0 & 0 & 0 \\
0 & 0 & 0 & 0 \\
0 & 0 & 0 & 0 \\
0 & 0 & 0 & 0 \\
1 & 0 & 1 & 0 \\
-m & 0 & mr & 0 \\
0 & 1 & 0 & 1 \\
0 & m & 0 & mr \\
v & 0 & 0 & 0 \\
0 & v & 0 & 0 \\
0 & 0 & rv & 0 \\
0 & 0 & 0 & rv
\end{bmatrix}$$

The state output vector, shaft position and velocity information at the magnetic bearings, is defined as

$$[\mathbf{y}]^t = [Y_1, Z_1, Y_2, Z_2, \dot{Y}_1, \dot{Z}_1, \dot{Y}_2, \dot{Z}_2],$$

so the [C] matrix is

$$\begin{bmatrix}
1 & -1 & 0 & 0 & 0 & 0 & 0 & 0 & 1 & 0 & 0 & 0 \\
0 & 0 & 1 & 1 & 0 & 0 & 0 & 0 & 0 & 1 & 0 & 0 \\
1 & r & 0 & 0 & 0 & 0 & 0 & 0 & 0 & 0 & 1 & 0 \\
0 & 0 & 1 & -r & 0 & 0 & 0 & 0 & 0 & 0 & 0 & 1 \\
0 & 0 & 0 & 0 & 1 & -1 & 0 & 0 & -1 & -w & 0 & 0 \\
0 & 0 & 0 & 0 & 0 & 0 & 1 & 1 & w & -1 & 0 & 0 \\
0 & 0 & 0 & 0 & 1 & r & 0 & 0 & 0 & -1 & -w & \\
0 & 0 & 0 & 0 & 0 & 0 & 1 & -r & 0 & 0 & w & -1
\end{bmatrix}$$

and the [D] matrix is

$$\begin{bmatrix}
0 & 0 & 0 & 0 \\
0 & 0 & 0 & 0 \\
0 & 0 & 0 & 0 \\
0 & 0 & 0 & 0 \\
v & 0 & 0 & 0 \\
0 & v & 0 & 0 \\
0 & 0 & rv & 0 \\
0 & 0 & 0 & rv
\end{bmatrix}$$